buildings

MDPI

Article

Settlement Behavior Analysis of Adjacent Existing Buildings Induced by Foundation Pit Construction in River Basin

Yanlu Zhao [1], Mingrui Cao [1], Zhigang Guo [1], Lifeng Zhang [2,*] and Erdi Abi [2]

[1] The Seventh Engineering Co. Ltd. of CCCC First Highway Engineering Cc. Ltd., Zhengzhou 451450, China; zyl_77@163.com (Y.Z.); 18883235569@163.com (M.C.); gzg_1018@163.com (Z.G.)
[2] National Engineering Research Center for Inland Waterway Regulation, Chongqing Jiaotong University, Chongqing 400074, China; abierdi@163.com
* Correspondence: zhlifeng0711@163.com

Abstract: The Yellow River Basin features a unique geographical environment with challenges like seawater erosion and soft soil. In this context, the construction of foundation pits can significantly impact the settlement of adjacent structures. Grounded in a real-world project, this study employs the finite element software Midas GTS to construct a 3D interaction model between foundation pit excavation and nearby buildings. Through this model, we analyze the settlement patterns of adjacent buildings influenced by variables such as foundation soil strength, slope gradient, and construction sequence. By integrating orthogonal experimental design and range analysis, we identify the sensitive factors affecting the settlement deformation and stability of foundation pits. Our analysis reveals that among the factors significantly influencing settlement deformation at the foundation pit base, groundwater levels and internal friction angles are the most critical. Slope gradient and soil cohesion also play substantial roles, whereas the compressive modulus of soil shows relatively less impact. However, a comparison with actual engineering data indicates that groundwater factors considerably affect slope deformation, underscoring the necessity for stringent control of groundwater level fluctuations.

Keywords: Yellow River Basin; foundation pit excavation; adjacent buildings; settlement law; sensitivity factors

check for updates

Academic Editor: Harry Far

Received: 16 May 2025
Revised: 27 May 2025
Accepted: 6 June 2025
Published: 10 June 2025

Citation: Zhao, Y.; Cao, M.; Guo, Z.; Zhang, L.; Abi, E. Settlement Behavior Analysis of Adjacent Existing Buildings Induced by Foundation Pit Construction in River Basin. *Buildings* **2025**, *15*, 1991. https://doi.org/10.3390/buildings15121991

Copyright: © 2025 by the authors. Licensee MDPI, Basel, Switzerland. This article is an open access article distributed under the terms and conditions of the Creative Commons Attribution (CC BY) license (https://creativecommons.org/licenses/by/4.0/).

1. Introduction

In practical engineering applications, the excavation of deep foundation pits inevitably induces stress changes in the surrounding soil and rock masses, which in turn exerts a certain influence on the settlement of adjacent existing structures. To safeguard the safety and stability of these structures, it is of paramount importance to investigate the settlement patterns of adjacent buildings during foundation pit construction. Numerous scholars have conducted extensive research in this area. Zhou Quan [1] refined the formulae and theoretical framework for calculating the displacement of soil outside the foundation pit and expanded its scope of application through the use of Matlab software. Tan Yin et al. [2] analyzed and synthesized the measurement deformation results caused by the excavation of the underlying tunnel foundation pit and used a two-stage analysis method to derive the calculation formula for additional stress and the deformation control equation for adjacent tunnels under the influence of the excavation. The research results showed that the theoretical calculation results had very little difference from the actual measured deformation of the underground tunnels, thereby confirming the accuracy and rationality of the theoretical calculation formulas. Huang [3] modeled pit excavation using FLAC3D

software and discussed its impacts on adjacent buildings, roads, and municipal pipelines. Dai Zilie et al. [4] used the SPH model to study the influence of different parameters on the movement behavior of landslides. The obtained results were well fitted with the experimental data, indicating that numerical simulation has good stability and accuracy in addressing fundamental research issues. In complex geological conditions, Wang Meng et al. [5] optimized the reasonable width of the narrow coal pillar in the along-the-striking roadway of the hard roof, revealing the critical mechanism of stress release and structural instability of the surrounding rock during underground excavation. By adjusting the geometric parameters, they alleviated stress concentration and formed a methodological echo by designing support parameters to inhibit soil deformation and protect adjacent buildings in foundation pit engineering. Zhou [6] proposed a coupling method of finite difference method (FDM) and discrete element method (DEM) based on representative volume element (REV), which is used to analyze the stability of tunnel-surrounding rock. By combining the advantages of continuous medium and discontinuous medium simulations, this method can accurately depict the rock fracture process and stress evolution laws. This method is also applicable to the study of the interaction between soil and support structure and the deformation and failure mechanism in foundation pit excavation, providing a cross-scenario efficient numerical analysis tool for the stability prediction of underground engineering. Wang et al. [7] developed similar materials with different tensile–compressive ratios to simulate the mechanical response of surrounding rock during tunnel-boring machine excavation, providing an experimental basis for optimizing tool parameters and geological adaptability. Zou et al. [8] systematically reviewed the multi-field coupling numerical simulation methods in deep rock mass fragmentation analysis, emphasizing the crucial role of cross-scale modeling techniques in predicting the cutting efficiency of TBM and the evolution of rock mass damage under complex geological conditions. The research indicates that the hybrid method combining the discrete element method and peridynamics can significantly enhance the accuracy of rock fragmentation simulation in soft and hard composite strata, providing theoretical support for optimizing TBM construction parameters. Chang et al. [9] revealed the deformation patterns of existing tunnels caused by the concurrent mechanized tunneling underpass construction through actual engineering cases and proposed a dynamic adjustment strategy for support parameters based on monitoring data. The study found that the interaction of tunnel groups led to a significant stress superposition effect. By combining numerical simulation to predict the deformation threshold, it provided empirical evidence for the risk control of collaborative construction of densely located tunnel clusters in cities. Ma et al. [10] revealed the pore collapse and ice crystal redirection mechanisms of the snow body under compressive load through microstructure characterization and established a snow body density–strength relationship model. This research provides a basis for optimizing mechanical parameters in polar engineering and avalanche protection structure design. Wu Nan [11] took the excavation of foundation pit groups adjacent to elevated rail transit structures as a case study and combined model tests with numerical simulation to investigate the impact of foundation pit group excavation on the deformation of adjacent structure foundations and control methods. In Yellow River basins, the unique geographical environment, characterized by issues such as seawater erosion and soft soil geology, makes the impact of foundation pit construction on the settlement of adjacent buildings more pronounced [12]. Therefore, studying the settlement patterns of adjacent buildings during foundation pit construction in coastal regions holds great practical significance for local construction projects. In this study, we combined practical engineering with numerical simulation to conduct an in-depth investigation into the settlement patterns of adjacent buildings during foundation pit construction in Yellow River basins and performed sensitivity analysis of

foundation pit settlement deformation and stability based on orthogonal experimental design, summarizing the significance of the effects of various influencing factors.

2. Model Establishment

To study the impact of the excavation of a large-scale foundation pit on the adjacent ground and buildings, a foundation pit excavation model was established using the finite element software Midas GTS NX to analyze the deformation of the surrounding ground. The finite element software Midas GTS has the following significant advantages in the modeling and analysis of ground deformation during foundation pit excavation and is particularly suitable for the detailed simulation of complex geotechnical engineering problems [13]. According to the actual engineering data, before the foundation pit was excavated, the distance between the foundation of the adjacent building under construction and the edge of the foundation pit was 43.7 m. During the excavation period, the upper structure of the bridge was constructed using the full-hall arch formwork cast-in-place method. The length of the foundation pit adjacent to the building is 197.4 m.

2.1. Model Establishment

To save computational time, improve efficiency, and facilitate timely adjustments to the model, an optimization analysis of the computational model was conducted. After optimizing the model length and the bottom length of the foundation pit, it was found that when the foundation pit length exceeds 50 m, the settlement value around the pit is slightly greater than that of the original excavation. Conversely, when the length is less than 50 m, the results are smaller than those of the original excavation. Therefore, the foundation pit length can be simplified to 50 m. Additionally, when the bottom length exceeds 50 m, the settlement value remains unchanged.

In conclusion, the size of the calculation model is simplified as follows: the distance between the bridge foundation under construction and the edge of the foundation pit is 50 m, the base length is 50 m, and the length of the foundation pit adjacent to the building is 173 m., as shown in Figure 1.

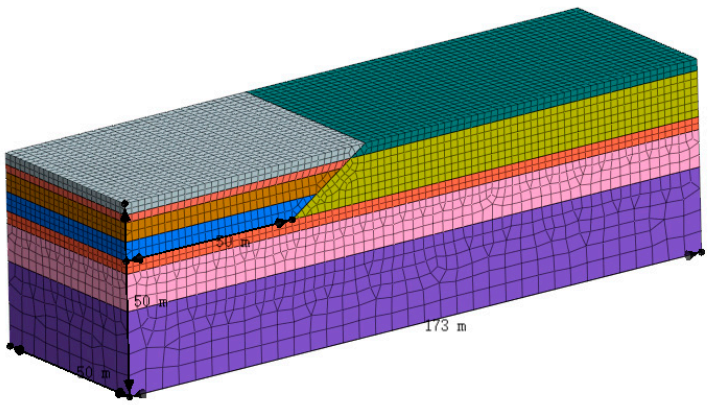

Figure 1. Simplified model diagram.

2.2. Constitutive Model Selection

In terms of the constitutive model, foundation pit excavation is an unloading process. The modified Mohr–Coulomb model, which is an improvement of the Mohr–Coulomb model, takes into account the changes in modulus during the unloading process of foundation pit excavation. Zhang Ruijin et al. [14] simulated foundation pit excavation using both the modified Mohr–Coulomb model and the Mohr–Coulomb model. By comparing the results with the monitoring data from the construction site, it was demonstrated that, in simulating foundation pit excavation, the modified Mohr–Coulomb model provides a

more accurate representation of the heave at the pit bottom and the settlement of the surrounding ground surface compared to the Mohr–Coulomb model. Therefore, the modified Mohr–Coulomb model is adopted in this study for simulation and calculation.

2.3. Parameter Selection

Based on the actual engineering conditions, the soil in the construction area, from top to bottom, consists of silt ①, silt ②, silt ③, silty clay, and clay. The soil constitutive model selected is the modified Coulomb–Mohr model. According to empirical values, the tangent stiffness of the soil Erefoed is equal to the secant stiffness Eref50, and both are twice the value of the compression modulus Es, that is, Erefoed = Eref50 = 2Es. The unloading modulus of the soil Erefur is three times the tangent stiffness Erefoed, that is, Erefur = Erefoed. The parameters for each soil layer are shown in Table 1 below:

Table 1. Soil Parameters.

Soil Layer	γ/ (kN/m^3)	C/kPa	Φ/(°)	Porosity	Horizontal Permeability Coefficient kx,y/(m/s)	Vertical Permeability Coefficient kz/(m/s)	Poisson's Ratio	Thickness/m	Es /kPa
Silt ①	18.7	11	26.5	0.875	2.4×10^{-4}	2.18×10^{-4}	0.3	3	11,400
Silt ②	19.3	10.5	26	0.755	2.4×10^{-4}	2.18×10^{-4}	0.3	12	11,750
Silt ③	18.9	115	27	0.828	8.1×10^{-5}	7.48×10^{-5}	0.3	3.3	11,030
Silty Clay	18.4	16.5	12	0.959	3.1×10^{-5}	8.7×10^{-6}	0.32	9.7	3710
Clay	17.8	18	15	1.163	8.6×10^{-5}	88×10^{-5}	0.33	22	4100

2.4. Boundary Settings

After the model is established, the bottom surface of the model is set as a fixed displacement boundary. The front, back, left, and right surfaces of the model are all set as fixed normal boundaries, and the top surface of the model is set as a free boundary.

2.5. Model Validation

During on-site construction of the foundation pit, the west slope was excavated by slope excavation, with an excavation depth of 15 m. The excavation was divided into three layers, each 5 m deep, and no support measures were implemented.

At the same time, several displacement monitoring points were set up about 10 m away from the top of the slope on the ground, as shown in Figure 2 to regularly monitor displacement deformation during the foundation pit excavation process. To avoid the spatial effect of displacement limitation caused by the foundation pit corners, the slope section with the ZSW03 monitoring point in the middle was selected for numerical simulation. The applicability of the established model was verified by comparing the displacement deformation from numerical simulation with the actual monitoring data.

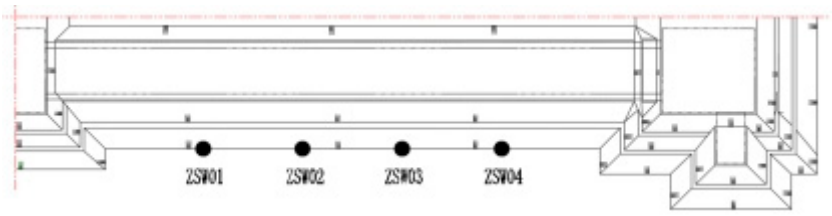

Figure 2. Layout of monitoring points on the sides in the direction of the foundation pit.

By comparing and analyzing the displacement deformation data collected on-site and the displacement deformation data obtained from the numerical simulation at the same points of the foundation pit, it was found that the maximum measured settlement of the foundation pit was 7.42 mm, while the maximum simulated settlement was

9.055 mm. The maximum measured horizontal displacement of the foundation pit was 8.9 mm, and the maximum simulated horizontal displacement was 10.11 mm, with a difference of 12.83%. The numerical simulation values [15] are larger than the actual deformations, but the difference between the two is relatively small. This indicates that the results obtained from the computational model are on the safe side. Therefore, the model can be used for the simulation calculations of this project.

3. Settlement Patterns of Adjacent Buildings Under Different Parameters

In foundation pit excavation, the main factors that affect the deformation and stability of the foundation pit are the cohesion of the soil, internal friction, compression modulus, excavation depth, slope ratio, and groundwater. This paper will study the settlement patterns of adjacent buildings under different parameters from four aspects: different foundation parameters, different slope ratios, different soil and rock elastic moduli, and different construction sequences.

3.1. Settlement of Adjacent Buildings Under Different Foundation Strengths

To analyze the impact of foundation soil parameters on the deformation of the surrounding soil during foundation pit excavation, the original soil parameters were reduced in a certain manner, and models were established for calculation respectively.

(1) Soil Parameters and Working Conditions

The reduction of soil parameters [16] is carried out to simulate different working conditions of soil parameters, and the reduction of soil parameters is according to the following formula:

$$c = \frac{c_0}{K} \tag{1}$$

$$\varphi = \arctan\left(\frac{\tan \varphi_0}{K}\right) \tag{2}$$

where c_0 is the initial soil cohesion in kPa; φ_0 is the initial internal friction angle in degrees; c, φ are the reduced cohesion and internal friction angle, respectively; and K is the reduction coefficient.

To cover a broad range of soil parameters, the K value is set to 0.5, 0.75, 0.96, 0.98, 1.02, 1.04, 1.25, and 1.5, making a total of nine values. A model is established for each K value for calculation, resulting in a total of nine models. The settlement and horizontal displacement of the ground within a certain range around the foundation pit are calculated for each model.

Figure 3 shows the ground settlement displacement from the edge of the foundation pit to 100 m away for each model after calculation. In the figure, when K equals 1, the soil in the model is the original soil. When K is less than 1, the soil strength parameters are greater than those of the original soil. When K is greater than 1, the soil parameters are less than those of the original soil. From the figure, it can be seen that when the K value is less than 1, the settlement value produced by the model is less than 13 mm. When the K value increases from 0.5 to 0.75, the change in settlement is very small, and the two settlement curves almost coincide. When the K value increases from 0.75 to 1, the settlement of the ground gradually increases. It can be concluded that when the soil parameters are about 1.3 times greater than those of the original soil, the change in settlement value of the surrounding soil is almost constant. When the soil parameters are less than 1.3 times those of the original soil, settlement gradually increases as the soil parameters approach those of the original soil.

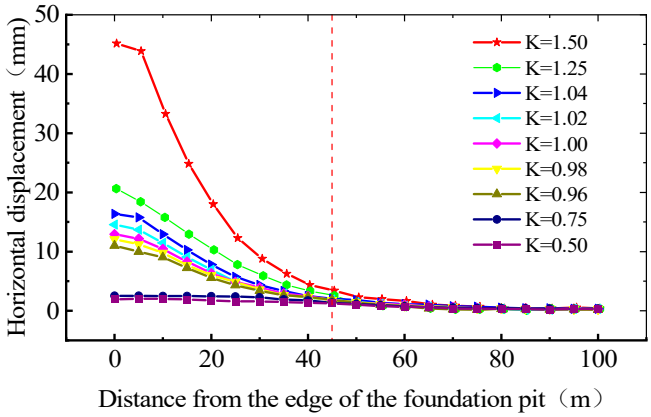

Figure 3. Settlement displacement of foundation pit surface under different soil strengths.

When the K value is greater than 1, the settlement of the soil around the foundation pit is greater than that of the original soil. As the K value increases from 1 to 1.25, the settlement of the soil gradually increases, but the magnitude of the increase is relatively small. When the K value increases from 1.25 to 1.5, settlement increases sharply. When K is 1.5, the maximum settlement around the foundation pit reaches 45 mm. This indicates that as the parameters decrease, the magnitude of the increase in settlement becomes larger and larger.

At the same time, in each model, when the distance between the ground and the edge of the foundation pit is greater than 45 m, the settlement of the surrounding ground is less than 3 mm. It can be concluded that in the several soil parameter models simulated this time, when the distance from the edge of the foundation pit is greater than 45 m, the impact of foundation pit excavation is relatively small.

The maximum values generated in each calculation model are selected for analysis, as shown in Figure 4. Maximum settlement increases with the increase of the reduction coefficient, and the magnitude of the increase also increases with the increase of the reduction coefficient [17]. The maximum values generated in each model are fitted using Origin 2024, and it is found that there is an exponential function relationship between the settlement value and the reduction coefficient, with the relationship as follows:

$$y = 1.89e^{2.17x} - 3.93 \quad (3)$$

$$R^2 = 0.975 \quad (4)$$

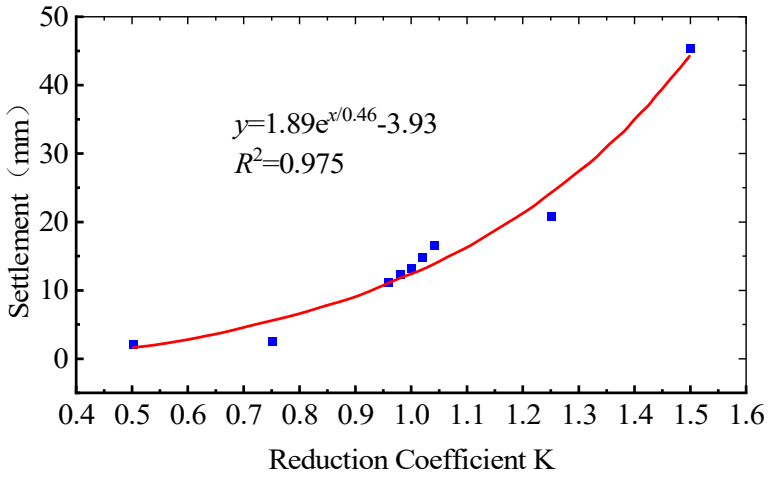

Figure 4. Trend chart of maximum settlement.

3.2. Settlement Patterns of Adjacent Buildings Under Different Slope Ratios

To analyze the impact of different excavation slope ratios on building deformation, foundation pit calculation models under different slope ratios were established for calculation and research. Among them, the slope ratio = the height of the slope/the horizontal projection length of the slope [18]. Three models were established. In these three models, the horizontal projection distance between the bottom of the foundation pit and the edge of the building was kept unchanged at 42 m. The building was simplified as a uniformly distributed load applied within the building range. The parameters of the established foundation pit models are shown in Table 2 below:

Table 2. Parameters of models with different excavation depths.

Model	Slope Ratio	Model Dimensions	Foundation Pit Depth (m)	Distance Between Foundation Pit and Building (m)
①	1:1.25	195 m × 50 m × 50 m	15	23.25
②	1:1.5	195 m × 50 m × 50 m	15	19.5
③	1:2	195 m × 50 m × 50 m	15	12

The models established under the three working conditions as shown in Table 2 are depicted in Figure 5.

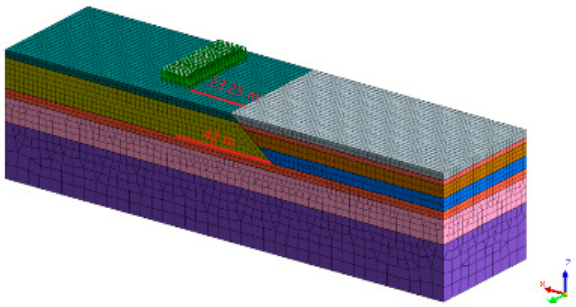

(**a**)

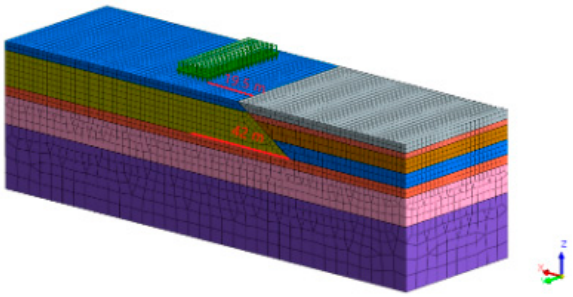

(**b**)

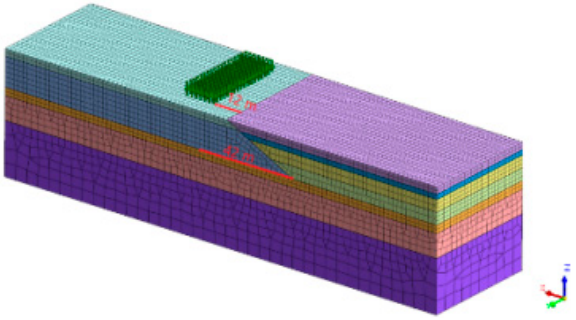

(**c**)

Figure 5. Computational model. (**a**) Slope Ratio 1:1.25; (**b**) Slope Ratio 1:1.5; (**c**) Slope Ratio 1:2.

Under the three working conditions, the maximum settlement values all occur at the location of the building adjacent to the foundation pit, which is the center of the loading area. As can be seen from Figure 6, the settlement values generated under these three working conditions also change with the variation of the slope ratio. The smaller the slope ratio, the greater the settlement value. This is because the smaller the slope ratio, the closer the building is to the edge of the foundation pit, and the greater the impact of foundation pit excavation. The simulation is consistent with reality. The maximum settlement value at the building location is greater than the settlement value at the edge of the foundation pit, mainly because the deformation at the building location is affected by both the loading and the foundation pit excavation, while the edge of the foundation pit is affected by the unloading of the foundation pit excavation and soil pressure [19]. After building construction, the ground has settled to a certain extent. Under the foundation pit excavation, additional settlement occurs. Therefore, the final settlement at the building location is greater than the settlement at the edge of the foundation pit. After the maximum settlement value appears, the settlement value decreases sharply with the increase of the distance from the edge of the foundation pit. Under the three working conditions, when the distance from the foundation pit exceeds 60 m, the settlement value of the adjacent ground is less than 3 mm.

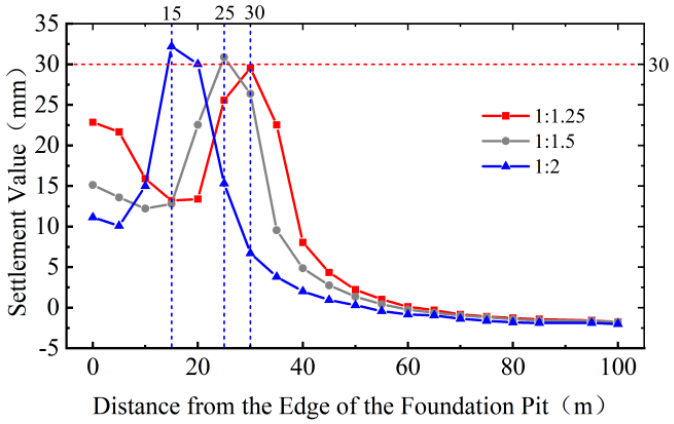

Figure 6. Settlement curves under different slope ratios.

3.3. Settlement Patterns of Adjacent Buildings Under Different Soil and Rock Elastic Moduli

To investigate the impact of elastic modulus on the deformation of the surrounding ground and buildings around the foundation pit, the model is set as a single-layer soil. According to the corresponding geological investigation data, different soils have different elastic moduli. Consider establishing a model for each soil layer for calculation, establishing five models, and the soil layer parameters for each model are shown in Table 3 below:

Table 3. Model soil parameters.

Model	Soil Layer	γ/(kN/m^3)	C/kPa	Φ/(°)	Porosity	Poisson's Ratio	Es/kPa
Model ①	Silt ①	18.7	11	26.5	0.875	0.3	11,400
Model ②	Silt ②	19.3	10.5	26	0.755	0.3	11,750
Model ③	Silt ③	18.9	115	27	0.828	0.3	11,030
Model ④	Silty Clay	18.4	16.5	12	0.959	0.32	3710
Model ⑤	Clay	17.8	18	15	1.163	0.33	4100

The foundation pit depth is 15 m, the slope ratio is 1:1.5, the distance between the edge of the foundation pit and the building is 19.5 m, and a uniform load of 60 kPa is applied to the ground to simulate the building. The computational model uses the

modified Coulomb–Mohr model, with parameters selected based on empirical values. The soil bottom boundary is a fixed boundary, the sides are fixed normal boundaries, and the top is a free boundary. The schematic diagram of the model is shown in Figure 7:

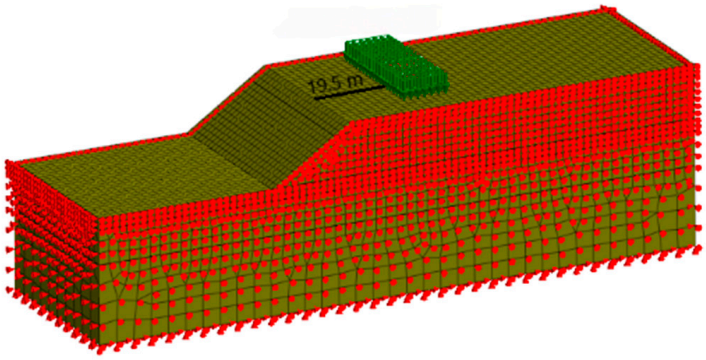

Figure 7. Schematic diagram of the model.

Through calculation, the settlement cloud diagrams and settlement data obtained from each model are organized to obtain the curves of settlement versus distance from the foundation pit edge for the five models, as shown in Figures 8 and 9. In models ①, ②, and ③, the three types of silt have small variations in compression modulus, and the resulting settlement differences are more pronounced within a certain range around the foundation pit edge. When the distance from the foundation pit is greater than 20 m, the settlement values of the three models show little difference, and the curves almost coincide. It can be seen from Figure 8 that the greater the compression modulus, the smaller the resulting settlement value. At the building location, the three models produce the same settlement value, and the curves are almost coincident. It can be concluded that when the compression moduli are not significantly different, the range of influence of different compression moduli is less than 20 m. The settlement changes at the foundation pit edge are more noticeable.

As shown in Figure 9, due to the very low compression modulus of silty clay and clay, the settlement is very significant. The settlement value of silty clay reaches around 510 mm, approximately 0.51 m, which indicates instability in practice. At the building location, the settlement exceeds 100 mm, surpassing the permissible limit. Therefore, when carrying out foundation pit excavation in these two types of soil, it is necessary to follow the specifications for calculation and design and to implement corresponding support measures.

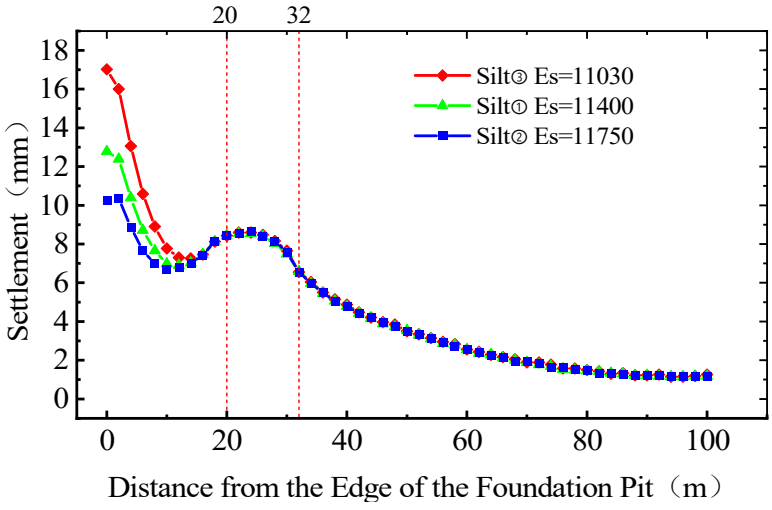

Figure 8. Settlement curves of silt models.

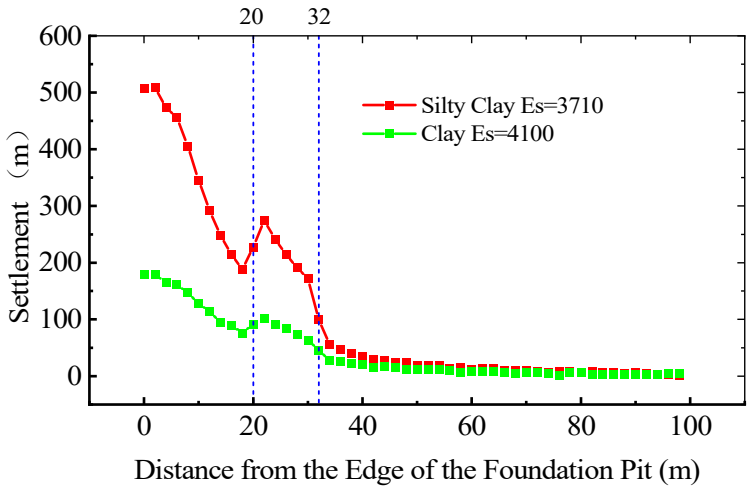

Figure 9. Displacement curves of silty clay and clay.

3.4. Settlement Patterns of Adjacent Buildings Under Different Construction Sequences

The model has dimensions of 173 m × 50 m × 50 m, with a foundation pit size of 50 m × 30 m and a depth of 15 m. During the foundation pit construction, slope excavation with a slope ratio of 1:1.5 is adopted. The bridge construction on-site is carried out using the full-hall scaffold cast-in-place method. Therefore, the bridge structure and scaffold loads are simplified as surface stresses applied to the ground, with an applied stress of 60 kN/m^2 over an area of 34 m × 12 m = 408 m^2. The distance between the edge of the scaffold adjacent to the foundation pit and the edge of the foundation pit is 20 m. The established model is shown in Figure 10.

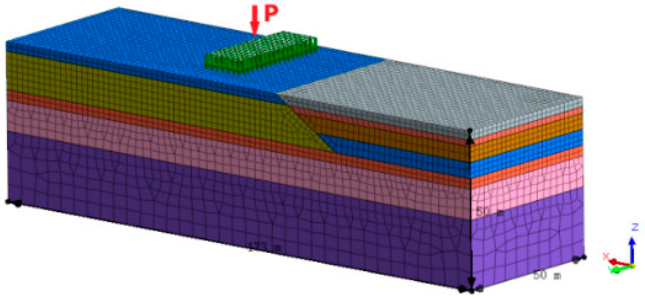

Figure 10. Foundation pit model diagram.

The bottom surface of the model is set as a fixed boundary. The two sides perpendicular to the x-axis in the model are set as fixed boundaries in the x direction, and the two sides perpendicular to the y-axis are set as fixed boundaries in the y direction. The top surface of the model is set as a free boundary [20].

The two construction sequences simulated are as follows:

Case ①: First-layer foundation pit soil excavation → Second-layer foundation pit soil excavation → Third-layer foundation pit soil excavation → Bridge scaffold construction

Case ②: Bridge scaffold construction → First-layer foundation pit soil excavation → Second-layer foundation pit soil excavation → Third-layer foundation pit soil excavation

Through simulation, the settlement of the foundation pit edge and the surrounding soil under the two working conditions was obtained. The settlement values of the two working conditions are plotted in the curve chart as shown in Figure 11. It can be seen from the figure that the difference in settlement values generated by the two working conditions is mainly at the scaffold position. At the edge of the foundation pit and in the range more than 40 m away from the edge of the foundation pit, the difference in settlement values generated in the two working conditions is very small.

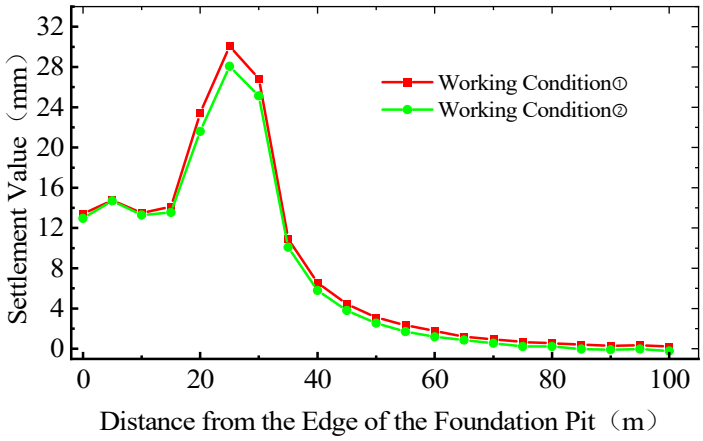

Figure 11. Settlement value curves.

From the settlement after excavation, it can be known that when there is building construction around the foundation pit, the settlement value at the building location will be greater if the building construction is carried out first followed by the foundation pit construction, compared with the situation where the foundation pit excavation is carried out first followed by the building construction. This is mainly because after the foundation pit construction is carried out first, the stress of the soil around the foundation pit is released and a certain deformation occurs. At the scaffold position, when the scaffold construction is carried out first, the ground within the scaffold range will settle to a certain extent due to the weight of the scaffold and the load it bears. After the foundation pit excavation, the deformation at the scaffold position will continue to increase. Therefore, the settlement value at the scaffold position in Case ① is greater than that in Case ②.

4. Sensitivity Analysis of Foundation Pit Settlement Deformation and Stability Based on Orthogonal Experimental Design

There are many factors that affect the stability of foundation pit slopes. In this paper, the cohesion, internal friction angle, unit weight, slope height, and slope ratio of the foundation pit soil are taken as the research objects, and a sensitivity analysis is conducted on these factors. Through analysis of the results of the orthogonal experiment, we can determine the importance of each factor, which can be categorized into key factors, important factors, general factors, and minor factors. Methods for analyzing the results of orthogonal experiments include range analysis (also known as intuitive analysis), variance analysis, analysis of interaction effects between factors, and trend level analysis [21]. We will use these four methods to analyze the correlation between the factors affecting slope stability and the slope safety factor.

4.1. Model Establishment

In this foundation pit simulation, the model has dimensions of 173 m × 50 m × 50 m, with a foundation pit bottom size of 50 m × 30 m. The model uses the same soil material, and the soil constitutive model adopts the modified Coulomb–Mohr model.

4.2. Selection of Orthogonal Table

In this case study, six factors that affect the stability of foundation pit slopes and the deformation around the foundation pit are investigated, namely, the slope ratio of foundation pit excavation (A), foundation pit depth (B), soil cohesion (C), internal friction angle (D), compression modulus (E), and groundwater level (F). Each factor is designed with five levels, as shown in Table 4 below:

Table 4. Levels of each factor.

Horizontal	Factors					
	A: Slope Ratio	**B: Depth /m**	**C: Cohesion /kPa**	**D: Internal Friction Angle/°**	**E: Compression Modulus/MPa**	**F: Groundwater Level**
1	1:1	5	10	10	2.5	None
2	1:1.25	10	15	15	5	−1
3	1:1.5	15	20	20	10	−2
4	1:2	20	25	25	20	−3
5	1:3	30	30	30	40	−4

After formulation of the factor level table, it is necessary to select an appropriate orthogonal table according to the research content, following these principles: ① Select the table based on the number of levels; ② Choose the table according to the characteristics of the experiment; and ③ Refer to the selection table to choose the table. In this study, there are six factors, each with five levels. Considering that interaction effect analysis will be conducted later, the L25 (5^6) orthogonal table is finally selected. The orthogonal experimental design calculation scheme is shown in Table 5 below:

Table 5. Orthogonal experimental design calculation scheme.

Experimental Groups	Factors					
	A	**B**	**C**	**D**	**E**	**F**
1	1	1	1	1	1	1
2	1	2	2	2	2	2
3	1	3	3	3	3	3
4	1	4	4	4	4	4
5	1	5	5	5	5	5
6	2	1	2	3	4	5
7	2	2	3	4	5	1
8	2	3	4	5	1	2
9	2	4	5	1	2	3
10	2	5	1	2	3	4
11	3	1	3	5	2	4
12	3	2	4	1	3	5
13	3	3	5	2	4	1
14	3	4	1	3	5	2
15	3	5	2	4	1	3
16	4	1	4	2	5	3
17	4	2	5	3	1	4
18	4	3	1	4	2	5
19	4	4	2	5	3	1
20	4	5	3	1	4	2
21	5	1	5	4	3	2
22	5	2	1	5	4	3
23	5	3	2	1	5	4
24	5	4	3	2	1	5
25	5	5	4	3	2	1

4.3. Orthogonal Experimental Results and Analysis

The stability results of the foundation pit slope and settlement deformation around the foundation pit obtained after calculation according to the orthogonal design sample scheme are shown in Table 6.

(1) Analysis of Stability Coefficient and Settlement Deformation

According to the "Technical Code for Building Slope Engineering" GB 50330-2013 [22], the safety grade of the foundation pit slope in this project is Grade I, and the slope stability safety factor Fst should not be less than 1.25. The stability coefficients of all experimental groups are plotted as shown below. From Figure 12, it can be seen that the stability coefficients obtained by experimental groups 2, 3, 4, 9, 10, 14, 18, 20, 23, and 24 are all less than the stability safety factor.

Table 6. Orthogonal experimental results (stability coefficient and settlement values).

Experimental Groups	Stability Coefficient F_S	Settlement Values/mm							
		0 m	5 m	10 m	20 m	30 m	40 m	50 m	60 m
1	1.40	55.35	36.03	25.02	11.34	3.90	0.07	−2.30	−3.57
2	1.11	−20.78	−28.95	−29.63	−32.65	−33.95	−33.48	−32.26	−30.76
3	1.10	−18.31	−25.56	−27.64	−30.05	−31.15	−31.16	−30.51	−29.44
4	1.13	−8.90	−16.02	−19.87	−23.42	−24.53	−24.66	−24.16	−23.30
5	5.80	−3.44	−8.15	−11.10	−14.40	−15.65	−16.04	−15.93	−15.54
6	2.30	6.15	3.03	1.40	−0.54	−1.51	−2.08	−2.38	−2.50
7	2.20	6.01	3.72	2.45	0.95	0.18	−0.27	−0.52	−0.65
8	1.61	−119.60	−182.67	−214.97	−249.76	−261.53	−264.80	−263.58	−261.78
9	0.80	−120	−200.00	−220.00	−250.00	−265.00	−270.00	−265.00	−265.00
10	0.80	−120	−200.00	−220.00	−250.00	−265.00	−270.00	−265.00	−265.00
11	3.43	−56.54	−60.44	−60.11	−56.37	−51.48	−46.67	−42.27	−38.48
12	5.90	4.99	0.39	−2.32	−5.22	−6.42	−6.76	−6.67	−6.39
13	1.74	11.47	7.45	4.86	1.80	0.17	−0.69	−1.16	−1.40
14	1.15	−7.05	−7.54	−7.52	−7.02	−6.31	−5.56	−4.86	−4.25
15	1.50	−75.23	−92.96	−99.04	−99.85	−92.94	−83.46	−73.98	−65.46
16	3.10	−3.21	−3.58	−3.61	−3.39	−3.03	−2.68	−2.37	−2.09
17	2.20	28.90	2.05	−14.46	−32.31	−41.43	−44.69	−45.50	−44.71
18	1.20	24.93	5.58	−5.35	−18.35	−24.62	−27.30	−28.30	−28.27
19	2.00	26.16	15.42	9.46	2.27	−1.38	−3.08	−4.04	−4.50
20	0.80	−120	−200.00	−220.00	−250.00	−265.00	−270.00	−265.00	−265.00
21	4.60	−38.95	−37.79	−35.24	−30.33	−25.58	−21.77	−18.48	−15.76
22	1.83	−17.70	−19.70	−20.34	−19.88	−18.67	−17.29	−15.78	−14.50
23	0.80	−120	−200.00	−220.00	−250.00	−265.00	−270.00	−265.00	−265.00
24	1.03	−74.09	−84.86	−85.35	−86.53	−85.41	−81.42	−76.02	−70.43
25	5.80	40.20	23.22	13.28	1.63	−4.44	−7.05	−8.41	−8.88

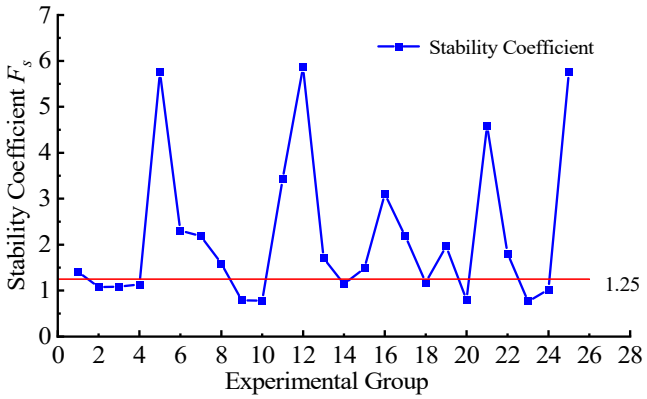

Figure 12. Comparison of stability coefficients.

By extracting the settlement values within the range of 0 m to 60 m from the edge of the foundation pit for each experimental group, the settlement curves generated by each test group are shown in Figure 13. It can be seen that among all the experimental groups, the settlement values within the range of 0 m to 60 m from the edge of the foundation pit

for experimental groups 6, 7, 23, 13, 14, and 16 are all within 10 mm. For experimental groups 1, 2, 8–11, 15, 17–21, and 23–25, the settlement values generated at the edge of the foundation pit are relatively large. Experimental groups 9, 10, 20, and 23 did not converge, resulting in the largest settlement values, which increase with distance from the edge of the foundation pit.

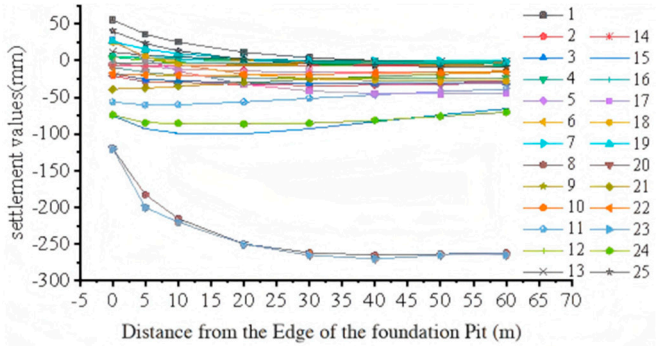

Figure 13. Settlement comparison chart.

(2) Range Analysis

Range analysis is relatively simple. When performing range analysis, first, calculate the sum of the results caused by each level of each factor, represented by K_{1j}, K_2j, K_{3j}, K_{4j}, K_{5j}. Second, calculate the range of the sums of the results caused by different levels, denoted by R_j. Finally, determine the sensitivity of the factors based on the size of the range. A larger range indicates a greater impact on the safety factor, meaning it is more sensitive. The range analysis is shown in Table 7.

Table 7. Range analysis of stability coefficient.

Factors	A: Slope Ratio	B: Depth /m	C: Cohesion /kPa	D: Internal Friction Angle/°	E: Compression Modulus/MPa	F: Groundwater Level
K_{1j}	10.538	14.8303	6.3758	9.7004	7.7473	13.1254
K_{2j}	7.7129	13.2313	7.7098	7.7632	12.3321	9.2723
K_{3j}	13.7035	6.4379	8.5567	12.5504	14.4035	8.3287
K_{4j}	9.301	6.1126	17.5444	10.6383	7.7817	8.3567
K_{5j}	14.0598	14.7031	15.1285	14.6629	13.0506	16.2321
R_j	6.3469	8.7177	11.1686	6.8997	6.6562	7.9034
Sensitivity Ranking	6	2	1	4	5	3

As can be seen from Table 7, the range values of the six factors are very close. The results show that among the six factors, the order of importance is cohesion > depth > groundwater level > internal friction angle > compression modulus > slope ratio. The stability coefficient of the slope is correlated differently with these six factors. It is positively correlated with the cohesion, internal friction angle, and compression modulus of the soil, increasing as they increase. It is negatively correlated with the depth and slope ratio of the foundation pit, decreasing as they increase. The presence or absence of groundwater and the depth of the groundwater level also have a significant impact on the stability of the foundation pit slope. The lower the groundwater level, the higher the stability coefficient.

The settlement values at the positions 0 m and 40 m away from the edge of the foundation pit are selected for range analysis. The range analysis tables are shown in Table 8.

As can be seen from the table, among the factors affecting the settlement of the foundation pit, the order of influence from greatest to least is as follows: groundwater level > slope ratio > internal friction angle > depth > cohesion > compression modulus. Therefore, during the foundation pit excavation process, the most severe factors affecting settlement

deformation are groundwater level, internal friction angle, slope ratio, and cohesion. The conclusions obtained through range analysis are consistent with the information obtained from on-site investigations.

Table 8. Range analysis of settlement values at 0 m from the edge of the foundation pit.

Factors	A: Slope Ratio	B: Depth /m	C: Cohesion /kPa	D: Internal Friction Angle/°	E: Compression Modulus/MPa	F: Groundwater Level
K_{1j}	3.92	−37.2	−64.47	−299.66	−184.67	139.19
K_{2j}	−347.44	1.42	−183.7	−206.61	−132.19	−306.38
K_{3j}	−122.36	−221.51	−262.93	49.89	−146.11	−234.45
K_{4j}	−43.22	−183.88	−86.52	−92.14	−128.98	−276.54
K_{5j}	−210.54	−278.47	−122.02	−171.12	−127.69	−41.46
R_j	351.36	279.89	198.46	349.55	56.98	445.57
Sensitivity Ranking	2	4	5	3	6	1

(3) Variance Analysis

Variance analysis assumes that each population is a normal variable with equal variances [23]. It tests whether the means of each group are consistent under the F hypothesis, thereby identifying whether the effects of each factor are significant. The significance level α is taken as 0.01 and 0.05. When $F \geq F0.05$, it is considered to be highly significant; when $F0.10 \leq F \leq F0.05$, it is considered to have a significant effect; when $F \leq F0.1$, the effect is considered to be less significant.

The variance analysis for the stability coefficient is shown in Table 9. By consulting the table, we can obtain F0.05(4, 4) = 6.39 and F0.10(4, 4) = 4.11.

Table 9. Variance analysis of stability coefficient.

Source of Error	Sum of Squares for Factor Deviations	Degrees of Freedom	Mean Square	F	Level of Significance
A	6.1113	4	1.52	40.74	Significant
B	15.6085	4	3.902	104.06	Significant
C	19.6064	4	4.902	130.71	Significant
D	5.6195	4	1.405	37.463	Significant
E	7.6962	4	1.924	51.308	Significant
F	9.7960	4	2.449	65.307	Significant
Error	0.1500	4	0.038		
Total Variation	64.5879	24			

It is worth comparing and finding that the six factors have a very significant impact on the stability of the foundation pit slope. The significance level has been quantified based on the F value. Further comparison of the significance differences among these six factors reveals that cohesion has the greatest significance, followed by excavation depth. The significance differences of groundwater, compression modulus, internal friction angle, and slope ratio are not very large, but their impact on the stability coefficient is still very significant. Table 10 shows the range analysis table of settlement values at a distance of 0 m from the edge of the foundation pit. The analysis results indicate that the factors with significant impact on the settlement deformation of the foundation pit bottom are groundwater, internal friction angle, depth, slope ratio, and cohesion. Among them, groundwater and internal friction angle have the most significant impact. Depth, slope ratio, and cohesion are relatively significant, while the compression modulus of the soil has a less significant impact.

The results of variance analysis are generally consistent with the conclusions obtained from range analysis, and the analysis results are also consistent with the on-site investigation.

Table 10. Range analysis of settlement values at 0 m from the edge of the foundation pit.

Source of Error	Sum of Squares for Factor Deviations	Degrees of Freedom	Mean Square	F	Level of Significance
A	15,664.1207	4	3916.030	12.743	Significant
B	11,646.7172	4	2911.679	9.475	Significant
C	5166.500136	4	1291.625	4.203	Not Significant
D	13,833.66158	4	3458.415	11.254	Significant
E	457.913536	4	114.478	0.373	Not Significant
F	28,565.26406	4	7141.316	23.238	Significant
Error	1229.2300	4	307.308		
Total Variation	76,563.4072	24			

During the foundation pit construction, displacement deformation monitoring was carried out at the top of the foundation pit slope, mainly monitoring settlement and horizontal displacement. In this project, due to the presence of adjacent buildings, a support method of three-axis mixing pile+bored pile+cap beam was used for protection on the side of the foundation pit close to the building. On the two sides in the direction of the foundation pit, only slope excavation was carried out without support. Monitoring data on both sides of the foundation pit were collected on-site. The monitoring cycle of the monitoring points is 10 days per time, and the monitoring points are set on the cap beam. The layout of the monitoring points is shown in Figure 14.

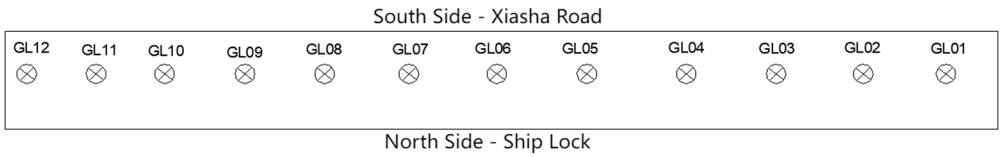

Figure 14. Layout of monitoring points at the top of the foundation pit slope.

The monitoring data on the sides in the direction of the foundation pit are shown in Figure 14, with a monitoring cycle of 10 days.

The collected cumulative deformation displacement data [24] of the foundation pit are plotted using Origin software. Figure 15 shows the cumulative settlement of each monitoring point in the foundation pit. It can be seen from the figure that the settlement generated by the monitoring points on the side close to the building is not large, all less than 10 mm, and tends to be stable over time. Overall, the settlement deformation is very small, indicating that the support structure has a good protective effect.

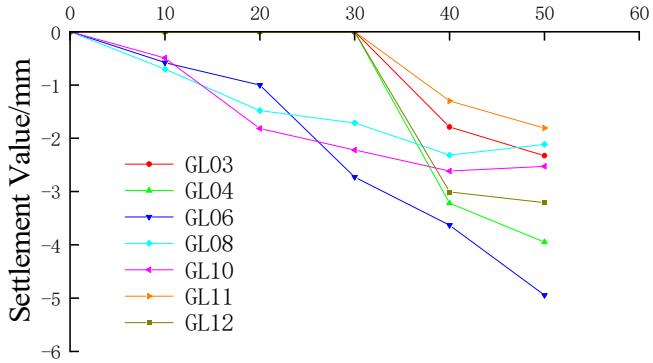

Figure 15. Cumulative settlement curves of monitoring points on the side close to the building.

Figure 16 shows the cumulative settlement curves of the monitoring points on the sides in the direction of the foundation pit. It can be seen from Figure 16 that after the foundation pit

construction began, deformation occurred, but with time, the change in cumulative settlement was very small, and the total settlement was very small, around 6 mm.

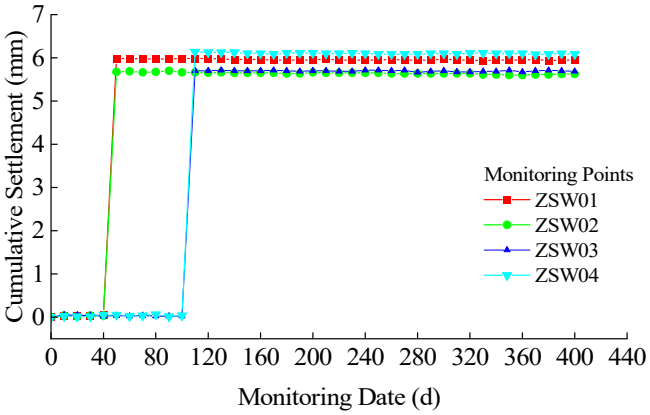

Figure 16. Cumulative settlement curves of monitoring points on the sides in the direction of the foundation pit.

The deformation generated without support is very small, indicating good soil properties [25]. At the construction site, due to the high groundwater level, after the foundation pit excavation, the groundwater was dynamically regulated and the changes in groundwater were monitored in real time. Timely dewatering was carried out to ensure the safety and stability of the slope. Therefore, the groundwater factor has a significant impact on slope deformation, which is consistent with the analysis results.

5. Conclusions

This research has achieved a breakthrough in the study of the impact of foundation pit construction in coastal areas on the settlement of adjacent buildings. It innovatively combines actual engineering with finite element simulation, systematically analyzes the settlement patterns under the combined effect of multiple factors and precisely identifies sensitive factors by means of orthogonal experiments, providing highly valuable guidance for engineering practice. The research team, on one hand, conducts detailed geological exploration to accurately obtain soil parameters and optimize the model; on the other hand, uses efficient numerical simulation technology to cross-verify with on-site monitoring data, continuously calibrating the model to ensure the reliability and applicability of the simulation results. In the future, by further expanding the research boundaries and integrating more actual engineering cases and long-term monitoring data, the research results are expected to be more universal and forward-looking, continuously deepening understanding and the application level in this field.

(1) The maximum settlement value increases with the increase in the reduction coefficient K, and the magnitude of the increase also increases with the increase of K. There is an exponential function relationship between the settlement value and the reduction coefficient K. This indicates that as the soil parameters decrease, the settlement will increase more and more significantly.

(2) The smaller the slope ratio, the greater the settlement value. This is because the smaller the slope ratio, the closer the building is to the edge of the foundation pit, and the greater the impact of foundation pit excavation. The maximum settlement value at the building location is greater than the settlement value at the edge of the foundation pit. When the distance between the building and the edge of the foundation pit reaches 60 m, the settlement impact is minimal.

(3) For different soil and rock elastic moduli, the magnitude of the elastic modulus has a smaller impact on the settlement of distant adjacent buildings but a greater impact

on the edge of the foundation pit. In particular, when excavating foundation pits in clay with low elastic modulus, slope support should be carried out according to the specifications.

(4) From the perspective of construction sequence, when there are adjacent building projects in foundation pit engineering, carrying out the construction of adjacent buildings first and then excavating the foundation pit can reduce the settlement of adjacent buildings.

(5) Through sensitivity analysis of the factors, it is found that among the factors significantly affecting the settlement deformation at the foundation pit bottom, groundwater and internal friction angle have the most significant impact. Depth, slope ratio, and cohesion also have a notable impact, while the compression modulus of the soil has a less significant effect. By comparing with the measured data from the engineering project, it is evident that the groundwater factor has a substantial impact on slope deformation, necessitating strict control of groundwater level changes to ensure slope safety.

Author Contributions: Methodology, Y.Z.; Software, M.C.; Resources, Z.G.; writing—review and editing, L.Z. and E.A. All authors have read and agreed to the published version of the manuscript.

Funding: This research was supported by the Science and Technology Research Project of CCCC First Highway Engineering Cc. Ltd. (KJYF-2025-7GS-01).

Data Availability Statement: The original contributions presented in the study are included in the article; further inquiries can be directed to the corresponding author.

Conflicts of Interest: Authors Yanlu Zhao, Mingrui Cao and Zhigang Guo were employed by the company The Seventh Engineering Co. Ltd. of CCCC First Highway Engineering Cc. Ltd. The remaining authors declare that the research was conducted in the absence of any commercial or financial relationships that could be construed as a potential conflict of interest.

References

1. Zhou, Q. Research on Foundation Deformation Calculation Analysis Based on Melan's Solution. *Sichuan Archit.* **2020**, *40*, 158–160+162.
2. Quan, Y.; Tan, X.; Hu, Z.; Huang, M. Measurement and Analysis of Deformation of Underlying Tunnel Induced by Foundation Pit Excavation. *Adv. Civ. Eng.* **2023**, *2023*, 8897139.
3. Huang, L. Numerical Simulation of Foundation Pit Excavation Impacts on Adjacent Infrastructure Using FLAC^{3D}. *J. Geotech. Eng.* **2023**, *45*, 45–58.
4. Dai, Z.; Lan, B.; Jiang, M.; Jiang, S. Numerical Modeling of Submarine Landslide Motion and Impact Behavior Based on the SPH Method. *J. Ocean. Univ. China* **2025**, *24*, 365–376. [CrossRef]
5. Wang, M.; Li, X.; Su, J.; Liu, W.; Fang, Z.; Wang, S.; Kang, J.; Yu, W. A study on the reasonable width of narrow coal pillars in the section of hard primary roof hewing along the air excavation roadway. *Energy Sci. Eng.* **2024**, *12*, 2746–2765.
6. Zhou, Z.; Gao, T.; Sun, J.; Gao, C.; Bai, S.; Jin, G.; Liu, Y. An FDM-DEM coupling method based on REV for stability analysis of tunnel surrounding rock. *Tunn. Undergr. Space Technol.* **2024**, *152*, 105917. [CrossRef]
7. Wang, J.; Zhang, Y.; Wang, K.; Li, L.; Cheng, S.; Sun, S. Development of similar materials with different tension-compression ratios and evaluation of TBM excavation. *Bull. Eng. Geol. Environ.* **2024**, *83*, 190. [CrossRef]
8. Zou, B.; Pei, C.; Chen, Q.; Deng, Y.; Chen, Y.; Long, X. Progress on Multi-Field Coupling Simulation Methods in Deep Strata Rock Breaking Analysis. *Comput. Model. Eng. Sci.* **2025**, *142*, 2457–2485.
9. Chang, J.; Thewes, M.; Zhang, D.; Huang, H.; Lin, W. Deformational behaviors of existing three-line tunnels induced by under-crossing of three-line mechanized tunnels: A case study. *Can. Geotech. J.* **2025**, *62*, 1–21. [CrossRef]
10. Ma, C.; Zheng, H.; Yang, N.; Sun, T.; Si, J.; Ren, D. Microstructural evolution and mechanical properties of snow under compression. *Constr. Build. Mater.* **2025**, *472*, 140883. [CrossRef]
11. Wu, N. Research on the Impact of Foundation Pit Group Excavation on the Deformation of Elevated Rail Transit Structure Foundations and Control Methods. Ph.D. Thesis, Beijing Jiaotong University, Beijing, China, 2021.

12. Jiang, X.; Zhao, Z.; Li, Y. Influence of shield tunnel construction on neighboring building. *J. Tianjin Univ.* **2008**, *41*, 725–730. (In Chinese)
13. Ding, R. Analysis and Countermeasures of the Impact of Deep Foundation Pit Construction on Adjacent Buildings. *Fujian Constr. Technol.* **2001**, 4–5+15.
14. Liu, F.; Xie, X. Analysis of the Impact of Subway Foundation Pit Enclosure Structure Trench Construction on the Settlement of Adjacent Buildings and Monitoring Data. *Chin. J. Rock Mech. Eng.* **2014**, *33*, 2901–2907.
15. Huang, H. Research on the Surface Settlement Law of Shallow Buried Tunneling Method in Shenzhen's Water-Rich Weak Strata. Master's Thesis, Beijing Jiaotong University, Beijing, China, 2010.
16. Zhang, C.; Zhang, D.; Han, K.; Wang, J. Study on Engineering Properties and Settlement Characteristics of Water-Rich Weak Strata in Shenzhen Metro after Excavation. *Mod. Tunneling Technol.* **2014**, *51*, 113–120.
17. Wei, J.; Cui, Y.; Shao, J. Three-Dimensional Finite Element Simulation of Groundwater and Ground Settlement in Jining City. *J. Chang. Univ. Sci. Technol.* **2000**, *30*, 376–381.
18. Ran, Q.; Gu, X. Ground Settlement Calculation Model of Fluid-Solid Coupling Considering Rheological Characteristics. *Chin. J. Geol. Disaster Prev.* **1997**, *9*, 99–103.
19. Yin, W. Research on Surface Settlement and Deformation Control Technology Caused by Shallow Buried Tunneling Construction in Water-Rich Weak Strata of Shenzhen Metro. Master's Thesis, Beijing Jiaotong University, Beijing, China, 2010.
20. Lei, G.; Han, F.; Xu, L. Analysis of Surface Settlement and Control Measures of Shield Tunnel in Water-Rich Gravelly Sand Layer. *J. Jilin Jianzhu Univ.* **2016**, *33*, 39–42+47.
21. Yang, X. Experimental Study on Settlement Characteristics of Recently Deposited Soil Foundation Under Water Level Fluctuation. Master's Thesis, Wuhan University of Science and Technology, Wuhan, China, 2013.
22. Yang, Z.; Wu, J.; Zhao, Y.; Li, B.; Du, J.; Tan, C. Finite Element Simulation and Monitoring Study on the Impact of Subway Deep Foundation Pit Excavation on Adjacent Buildings. *J. Build. Sci. Eng.* **2016**, *33*, 121–126.
23. *GB 50330—2013*; Ministry of Housing and Urban-Rural Development of the People's Republic of China, General Administration of Quality Supervision, Inspection and Quarantine of the People's Republic of China. Technical Code for Building Slope Engineering. China Architecture & Building Press: Beijing, China, 2014.
24. Liu, C. Research on the Impact of Deep Foundation Pit Excavation Support Methods in Water-Rich Areas on Adjacent Buildings. Master's Thesis, Xi'an University of Science and Technology, Xi'an, China, 2009.
25. Attewell, P.B.; Yeates, J.; Selby, A.R. *Soil Movement Induced by Tunneling and Their Effects on Pipelines and Structures*; Chapman & Hall: Glasgow, UK, 1986.

Disclaimer/Publisher's Note: The statements, opinions and data contained in all publications are solely those of the individual author(s) and contributor(s) and not of MDPI and/or the editor(s). MDPI and/or the editor(s) disclaim responsibility for any injury to people or property resulting from any ideas, methods, instructions or products referred to in the content.